
Dynamical Aspects of Shallow Sea Fronts

C. J. R. Garrett and J. W. Loder

Phil. Trans. R. Soc. Lond. A 1981 **302**, 563-581

doi: 10.1098/rsta.1981.0183

Email alerting service

Receive free email alerts when new articles cite this article - sign up in the box at the top right-hand corner of the article or click [here](#)

To subscribe to *Phil. Trans. R. Soc. Lond. A* go to: <http://rsta.royalsocietypublishing.org/subscriptions>

Dynamical aspects of shallow sea fronts

BY C. J. R. GARRETT† AND J. W. LODER‡

† *Department of Oceanography, Dalhousie University, Halifax, Nova Scotia B3H 4J1, Canada*‡ *Woods Hole Oceanographic Institution, Woods Hole, Massachusetts 02543, U.S.A.*

We examine the role of internal friction in the evolution of a two-dimensional front in a rotating stratified fluid. For a two-layer fluid with interfacial friction the depth of the frontal interface satisfies a diffusion equation with respect to time and the cross-frontal coordinate. Similarity solutions are used to compare the behaviour of the front for linear and quadratic interfacial friction laws. For a continuously stratified front a simple formula is derived for the cross-frontal flow induced by friction, parametrized in terms of an eddy viscosity coefficient A_V , provided that the Rossby and Ekman numbers are small. Outside surface and bottom Ekman layers the depth $z(x, \rho, t)$ of an isopycnal with density ρ satisfies the diffusion equation $z_t = [(N^2/f^2) A_V z_x]_x$, where N, f are the Väisälä and Coriolis frequencies, x is the cross-frontal coordinate and t is time. The consequences of this for the evolution and maintenance of a front are discussed. The circulation in tidal mixing fronts is examined, with results being presented for a semi-analytic diagnostic model, which is fitted to two particular continental shelf fronts. A prominent feature is a two-cell circulation pattern in the plane normal to the front. A variety of cross-frontal transfer mechanisms are discussed, with order-of-magnitude comparisons of their importance being made. Transfer by the mean flow appears to be more important than either shear flow dispersion or the flux associated with baroclinic eddies, but the results are sensitive to the parametrization of vertical mixing of momentum.

1. INTRODUCTION

Regions of much larger than average horizontal gradients of oceanic properties are well documented features of continental shelf seas. Prominent examples are the fronts between well mixed and stratified water in tidally energetic areas, the fronts between different water masses typically found at the continental shelf break and the fronts associated with the surfacing of the pycnocline in response to wind-driven coastal upwelling.

The presence of such fronts is not usually a surprise, and their location can often be explained quantitatively (as for tidal mixing fronts with the criterion of Simpson & Hunter (1974)). However, the circulation in fronts and its role in frontal maintenance and biological productivity are still very uncertain, as are the mechanisms and rates of cross-frontal transfers of water properties.

For many fronts the basic dynamical balance may well be geostrophic, with the vertical shear of current along the front related to the density gradient across the front. However, further considerations are required for the interpretation or prediction of cross-frontal gradients of the flow parallel to the front, or for an understanding of the cross-frontal flow that will maintain or modify an existing density structure.

The main goals of this paper will be to examine the cross-frontal flow induced by internal frictional processes, to examine the implications of predicted flow patterns, and to compare various possible mechanisms for cross-frontal transfer.

2. THE EFFECT OF FRICTION ON A FRONTAL INTERFACE

As a preliminary problem to demonstrate the role of friction in a rotating system we consider the situation illustrated in figure 1. A sloping interface at $z = -h(x, t)$ separates two fluids that differ in density by $\Delta\rho$. If the lower layer is assumed to be at rest, the free surface of the fluid of density ρ is elevated by an amount $(\Delta\rho/\rho)h$ above a geopotential at $z = 0$. This is dynamically crucial, but unimportant in our discussion of mass balance if $\Delta\rho \ll \rho$, as we assume.

If the upper layer is in geostrophic motion away from the interface its speed is given by the Margules formula

$$V = g'f^{-1}\partial h/\partial x, \quad (2.1)$$

where g' is the reduced gravity $g(\Delta\rho/\rho)$. This speed will be reduced close to the interface, where an interfacial stress τ will result in equal and opposite Ekman fluxes τ/f in the two layers (Csanady

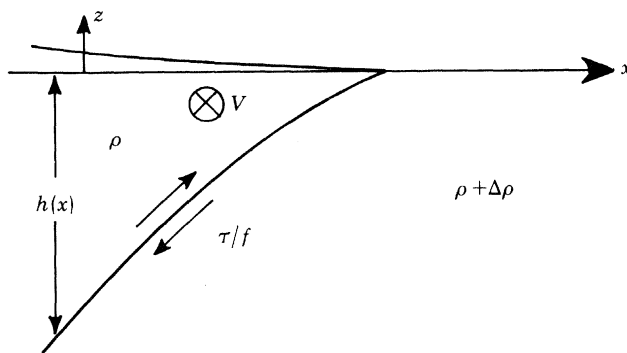


FIGURE 1. Schematic diagram of a front between two water masses of densities ρ and $\rho + \Delta\rho$.

1972, unpublished), as illustrated in figure 1. Convergences or divergences in this Ekman flux lead to changes in the depth of the upper layer according to the equation

$$\partial h/\partial t = -\partial(\rho^{-1}\tau f^{-1})/\partial x, \quad (2.2)$$

where we have taken τ to be the y -component of stress on the upper layer; $-\tau$ is the stress exerted on the lower layer.

If the stress is linearly proportional to V , as for laminar flow of a fluid of constant viscosity, say $\tau = -\lambda V$, then (2.2) becomes

$$\partial h/\partial t = \lambda g'(\rho f^2)^{-1}\partial^2 h/\partial x^2 \quad (2.3)$$

which is simply a diffusion equation describing the lateral spread of the lighter fluid over the top of the denser fluid. This result was derived by Stommel & Fedorov (1967) for the similar problem of the lateral spread of an intrusion in the interior of a fluid. They also derived a diffusion-like equation when the Ekman depth is not (as we have assumed here) much less than the depth of the spreading layer.

In any geophysical application it is probably more appropriate to parametrize the interfacial stress with the quadratic drag law

$$\tau = -C_D\rho V|V|, \quad (2.4)$$

where, according to Csanady (1978, 1980), values between 0.3×10^{-3} and 0.5×10^{-3} are appropriate for the drag coefficient C_D .

Substitution of (2.4) into (2.2) leads to

$$\frac{\partial h}{\partial t} = C_D g'^2 f^{-3} \frac{\partial [|\partial h / \partial x| (\partial h / \partial x)]}{\partial x}, \quad (2.5)$$

which is the diffusion equation with variable diffusivity. The rate at which the front decays, owing to lateral spreading of the upper layer, decreases with time.

One important point is that whatever form is taken by the interfacial stress, and whatever the ratio of Ekman depth to upper layer depth, the lateral flux in the top layer is equal and opposite to the flux in the lower layer provided that the stress at the free surface is zero. Any divergence in the upper Ekman layer is balanced by convergence in the lower Ekman layer, and there is no need to invoke, as did Tang (1980), upwelling in the lower layer. (Actually the above statements are slightly imprecise. The mass flux τ/f is equal and opposite so that the volume flux $\tau/\rho f$ is slightly greater in the upper layer. This discrepancy allows for a simultaneous adjustment of free surface elevation as well as interfacial depth).

2.1. Similarity solutions

Equations (2.3) and (2.5) could be used to predict the evolution of some initial shape of the interface (and are perhaps more immediately relevant, in their axisymmetric form, to a study of Gulf Stream ring decay than to shallow water fronts). A variety of mathematical techniques are, of course, available for the solution of the linear diffusion equation, but the nonlinearity of (2.5) makes it much less tractable. However, the difference between solutions of (2.3) and (2.5) can be clearly illustrated by comparing the similarity solutions for the spread of a δ -function of area $Q = \int_{-\infty}^{\infty} h(x, t) dx$. For (2.3), with $\lambda g'(\rho f^2)^{-1}$ denoted by K , the well known solution is

$$h(x, t) = Q(4\pi Kt)^{-\frac{1}{2}} \exp[-x^2(4Kt)^{-1}]. \quad (2.6)$$

For (2.5), dimensional analysis (in which we must treat h as having a dimension other than length) leads to

$$h(x, t) = Q(K'Qt)^{-\frac{1}{4}} F(\xi), \quad (2.7)$$

where $K' = C_D g'^2 f^{-3}$ and $\xi = x(K'Qt)^{-\frac{1}{4}}$. The differential equation satisfied by $F(\xi)$ is

$$\frac{1}{4} \left(F + \xi \frac{dF}{d\xi} \right) = - \frac{d[|dF/d\xi| (dF/d\xi)]}{d\xi}. \quad (2.8)$$

Symmetry about $\xi = 0$ and finiteness of F require $dF/d\xi = 0$ at $\xi = 0$, so that the first integral of (2.8) is

$$\frac{1}{4} \xi F = - |dF/d\xi| (dF/d\xi). \quad (2.9)$$

We require $F \geq 0$ so that $dF/d\xi \leq 0$ for $\xi > 0$, and (2.9) becomes

$$\frac{1}{4} \xi F = (dF/d\xi)^2 \quad (2.10)$$

and

$$F = \frac{1}{3\sqrt{6}} (\xi_0^{\frac{3}{2}} - \xi^{\frac{3}{2}})^2 \quad \text{for } \xi < \xi_0. \quad (2.11)$$

The solution for $\xi < 0$ is obtained by writing $-\xi$ for ξ in (2.11), and the condition $\int_{-\xi_0}^{\xi_0} F(\xi) d\xi = 1$ gives $\xi_0 = 2.52$ and $F(0) = 0.44$.

The solution with quadratic friction differs from that with linear friction by decaying like $t^{-\frac{1}{4}}$ instead of $t^{-\frac{1}{2}}$. More importantly, with quadratic friction the front meets the surface at a finite value of x , instead of approaching it asymptotically as $x \rightarrow \infty$. (In fact the work of Stommel &

Fedorov (1967) indicates that this effect could be due to a reduction in lateral flux as the depth of the upper layer becomes comparable with the Ekman depth.) The front is parabolic in shape near its intersection with the surface at $x = x_0 = \xi_0(K'Qt)^{\frac{1}{2}}$, with

$$h(x, t) = \frac{1}{16}\xi_0 Q(K'Qt)^{-\frac{3}{2}}(x_0 - x)^2, \quad (2.12)$$

which can be written

$$h(x, t) = \frac{1}{4}K'^{-1}(dx_0/dt)(x_0 - x)^2. \quad (2.13)$$

This local part of the similarity solution should develop rapidly from any initial distribution of h . In particular we notice that the rate of advance of the surface position of the front is

$$dx_0/dt = 4C_D g'^2 f^{-3} h(x, t) (x_0 - x)^{-2}. \quad (2.14)$$

With $C_D = 4 \times 10^{-4}$, $g' = 10^{-2} \text{ m s}^{-2}$ (for $\Delta\rho/\rho = 10^{-3}$), $f = 10^{-4} \text{ s}^{-1}$ and $h = 50 \text{ m}$ at $x_0 - x = 10 \text{ km}$ as rather arbitrarily chosen values, this gives $dx_0/dt = 0.08 \text{ m s}^{-1}$ for the instantaneous rate of advance of the front, a value that does not seem too implausible.

The neglect of density diffusion and the assumption of a sharp frontal interface obviously make it difficult to apply the above theory in any practical situation, but it may provide some guidance. In particular it does demonstrate that the basic role of friction is to allow for lateral spread of a frontal interface and so reduce the geostrophic current.

Before passing on to a discussion of the role of friction in a continuously stratified front it seems worth while to complete this section by giving the axisymmetric solutions corresponding to (2.6) and (2.11). The basic equation (2.2) is replaced by

$$\partial h/\partial t = -r^{-1} \partial(r\rho^{-1}\tau f^{-1})/\partial r \quad (2.15)$$

with a similarity solution for linear friction

$$h(r, t) = Q(4\pi Kt)^{-1} \exp[-r^2(4Kt)^{-1}], \quad (2.16)$$

where $Q = \int_0^\infty 2\pi r h(r, t) dr$. For quadratic friction the solution is

$$h(r, t) = \frac{1}{45} Q(K'Qt)^{-\frac{2}{3}} (\eta_0^{\frac{3}{2}} - \eta^{\frac{3}{2}})^2, \quad (2.17)$$

with $\eta = r(K'Qt)^{-\frac{1}{2}}$ and $\eta_0 = 2.23$, showing a spreading rate proportional to $t^{\frac{1}{2}}$ as opposed to $t^{\frac{1}{3}}$ for linear friction, and again giving an interception of the front with the surface at a finite radius. The solution near the surface position of the front, and the rate of advance of this position, are exactly as in (2.13) and (2.14) with x, x_0 replaced by r, r_0 .

3. DECAY OF A CONTINUOUSLY STRATIFIED FRONT

We now progress to a situation in which the density is a continuous function of x and z , but still assume that the flow is independent of the coordinate y along the front. If we ignore friction the flow along the front satisfies the thermal wind equation

$$\partial v/\partial z = -gf^{-1}\rho^{-1} \partial\rho/\partial x \quad (3.1)$$

if we make the usual assumption of ignoring $v \partial\rho/\partial z$ compared with $\rho \partial v/\partial z$.

We assume that vertical transfer of momentum can be parametrized in terms of an eddy viscosity coefficient A_{∇} and wish to examine the way in which this leads to a weak cross-frontal flow. The governing equations are

$$\partial u/\partial t + u \partial u/\partial x + w \partial u/\partial z - fv + \rho^{-1} \partial p/\partial x = \partial(A_{\nabla} \partial u/\partial z)/\partial z, \quad (3.2)$$

$$\partial v/\partial t + u \partial v/\partial x + w \partial v/\partial z + fu = \partial(A_{\nabla} \partial v/\partial z)/\partial z, \quad (3.3)$$

$$\rho^{-1} \partial p/\partial z + g = 0, \quad (3.4)$$

$$\partial \rho/\partial t + u \partial \rho/\partial x + w \partial \rho/\partial z = 0, \quad (3.5)$$

$$\partial u/\partial x + \partial w/\partial z = 0, \quad (3.6)$$

where we assume a hydrostatic balance in the vertical direction, and ignore the diffusion of density as well as horizontal diffusion of momentum. Taking u, v, w to have scales U, V, W , and significant variations in the velocity field to occur over horizontal and vertical distances L, H , we assume $V/L \ll f$ and $A_{\nabla} \ll fH^2$ (i.e. small Rossby number and small Ekman number). These assumptions mean that the first three terms in (3.2) and (3.3) are negligible, and that the viscous term is also negligible in (3.2). Hence we may substitute on the right-hand side of (3.3) the geostrophic shear from (3.1), and obtain

$$u = -gf^{-2}\rho^{-1} \partial(A_{\nabla} \partial \rho/\partial x)/\partial z. \quad (3.7)$$

The continuity equation (3.6) then gives

$$w = gf^{-2}\rho^{-1} \partial(A_{\nabla} \partial \rho/\partial x)/\partial x + L(x), \quad (3.8)$$

where $L(x)$ is an arbitrary function of x . These equations for flow in the cross-frontal plane were derived by Garrett & Horne (1978) who pointed out that $L(x) = 0$ if $A_{\nabla} = 0$ at the free surface. If $A_{\nabla} \neq 0$ either at the free surface or at the bottom (assumed flat), then it will not in general be possible to choose $L(x)$ to give $w = 0$ at both boundaries. This problem draws attention to the fact that (3.7) and (3.8) are not valid within surface and bottom Ekman layers, with thickness of order $(A_{\nabla}/f)^{\frac{1}{2}}$.

However, integrating (3.3) across a surface Ekman layer, with $A_{\nabla} \partial v/\partial z = 0$ at the surface and $\partial v/\partial z$ given by (3.1) at the base of the layer, we obtain an Ekman flux $gf^{-2}\rho^{-1}A_{\nabla} \partial \rho/\partial x$. Thus the vertical velocity in the interior can feed the Ekman flux divergence if $L(x) = 0$. We conclude that (3.7) and (3.8), with $L(x) = 0$, are valid in the fluid interior.

We now examine the evolution of the density field in response to the cross-frontal flow given by (3.7) and (3.8). The density equation becomes (with subscripts t, x, z to denote differentiation)

$$\rho_t - gf^{-2}\rho^{-1}[A_{\nabla} \rho_x]_z \rho_x - (A_{\nabla} \rho_x)_x \rho_z = 0. \quad (3.9)$$

Gill (1981) pointed out that for a small perturbation from a state of uniform stratification the vertical advection dominates horizontal advection, and (3.9) resembles the equation for horizontal diffusion, with diffusivity $(N^2/f^2) A_{\nabla}$, where $N^2 = -(g/\rho) \partial \rho/\partial z$. We go further by noting that in general (3.9) may be written, after division by $-\rho_z$, as

$$z_t = gf^{-2}\rho^{-1}[(A_{\nabla} \rho_x)_x + (A_{\nabla} \rho_x)_z z_x], \quad (3.10)$$

where $z_t = -\rho_t/\rho_z$ and $z_x = -\rho_x/\rho_z$ are respectively the rate of change of depth, and the slope, of an isopycnal surface. With the Boussinesq assumption this may be written

$$z_t = [(N^2/f^2) A_{\nabla} z_x]_x + [(N^2/f^2) A_{\nabla} z_x]_z z_x, \quad (3.11)$$

in which x, z, t are still the independent coordinates. However, if we now regard the depth z of an isopycnal as a function of x, ρ, t , (3.11) becomes

$$z_t = [(N^2/f^2) A_{\nabla} z_x]_x \quad (3.12)$$

where the x derivatives are for ρ, t constant.

This remarkable result shows that, even for variable stratification and variable viscosity, the depth of an isopycnal satisfies a horizontal diffusion equation, with variable horizontal diffusivity $(N^2/f^2) A_{\nabla}$.

Equation (3.12) may be derived alternatively by a formal change to density coordinates, with $z(x, \rho, t)$ the depth of a particular isopycnal, by proceeding from

$$\rho = \rho[x, z(x, \rho, t), t]. \quad (3.13)$$

Differentiation with respect to each of the three variables x, ρ, t , the other two being kept fixed, leads to

$$1 = \rho_z z_{\rho}, \quad 0 = \rho_x + \rho_z z_x, \quad 0 = \rho_t + \rho_z z_t. \quad (3.14)$$

Differentiation of the second of these equations with respect to x , with ρ, t constant, and with respect to ρ with x, t constant, provides terms suitable for substitution into (3.9), which may then be manipulated into the form of (3.12).

3.1. Frontal scales

In the absence of density diffusion (3.12) shows that the time-scale for the decay of a continuously stratified front is $T = (f^2/N^2) L^2/A_{\nabla}$, where L is a horizontal scale. For a front on the continental shelf we take $f^2/N^2 = 10^{-4}$ and $L = 10$ km. Appropriate values for A_{∇} are not really known, although some of the parametrizations in terms of parameters such as the tidal current and stratification will be discussed later. For the moment we merely point out that $T = 10^6$ s ≈ 10 days for $A_{\nabla} = 10^{-2}$ m²s⁻¹, but is nearer 3 months if $A_{\nabla} = 10^{-3}$ m²s⁻¹.

We may add a term $(K_{\nabla}\rho_z)_z$ to the right-hand side of (3.9) to represent the diffusion of density. If this, together with suitable boundary conditions, were to permit a steady state (though this is by no means clear), then the ratio of horizontal scale L to vertical scale H should be

$$L/H \approx (N/f) (A_{\nabla}/K_{\nabla})^{1/2}. \quad (3.15)$$

We note that this scale, determined mainly from diffusive arguments, is larger by a factor $(A_{\nabla}/K_{\nabla})^{1/2}$ than the scale N/f associated with vorticity arguments (see, for example, Pedlosky 1979).

With respect to independent coordinates x, ρ, t , the term $(K_{\nabla}\rho_z)_z$ may be written $(K_{\nabla}z_{\rho}^{-1})_{\rho}z_{\rho}^{-1}$, so that (3.12) becomes

$$z_t = [A_{\nabla}(N^2/f^2) z_x]_x - (K_{\nabla}z_{\rho}^{-1})_{\rho} \quad (3.16)$$

$$= [A_{\nabla}(N^2/f^2) z_x]_x - (K_{\nabla}z_{\rho}^{-2}z_{\rho})_{\rho}. \quad (3.17)$$

In these equations the first term on the right-hand side tends to diffuse away gradients of $z(x, \rho, t)$ along isopycnals, as already discussed, and the second term can be thought of as a

diffusion of z across isopycnals with a diffusivity $-K_V z_\rho^{-2}$, i.e a tendency to sharpen gradients of z in the cross-isopycnal direction. However, it is not clear that this equation sheds any light on the problem of frontal maintenance.

3.2. *Frontogenesis and frontolysis*

We can at least use (3.12) to make some remarks about the tendency of the frictionally induced flow to either enhance or weaken the horizontal density gradient. We note that the horizontal diffusion rate of a particular isopycnal is given by the local value of $(N^2/f^2) A_V$. Unless A_V is suppressed by vertical stability by a factor that increases faster than N^2 , there will thus be a tendency for the maximum lateral diffusion to occur in the most stably stratified part of the front. Near the surface this will lead to a sharpening of the horizontal density gradient, or frontogenesis, on the denser side of a front, and a weakening of the gradient, or frontolysis, on the less dense side.

This conclusion is only valid below a surface Ekman layer, which has a flux given by $A_V g f^{-2} \rho^{-1} \rho_x$ evaluated at the base of the Ekman layer. Depending on A_V this will tend to have a maximum in the vicinity of the front, and so, as for the flow below the Ekman layer, will tend to produce convergence on the denser side of the front.

3.3. *Summary*

The main conclusions of this section may be summarized as follows.

- (i) For low Rossby number and low Ekman number flows, and on the assumption of a parametrization of turbulent momentum transport in terms of an (variable) eddy viscosity, the horizontal component of the cross-frontal flow, outside surface and bottom Ekman layers, is given by the simple formula (3.7) involving the eddy viscosity A_V and density gradients.
- (ii) A simple formula for the vertical component of the velocity follows from the continuity equation.
- (iii) Outside surface and bottom Ekman layers, the equation for the advective evolution of the density field may be manipulated to show that an isopycnal surface satisfies the horizontal diffusion equation with diffusivity $(N^2/f^2) A_V$.
- (iv) As well as elucidating the physical effects of internal friction, this equation permits scale estimates of a decay time or the aspect ratio $(N/f) (A_V/K_V)^{1/2}$ to be expected in a front in which density advection is balanced by diffusion with vertical diffusivity K_V . However, the details of frontal evolution or maintenance require further work.
- (v) Regions of frontolysis and frontogenesis are to be expected near the surface outcropping of a front. The details are dependent on the parametrization of A_V , but frontogenesis is expected on the denser side of the front.

4. CIRCULATION IN TIDAL MIXING FRONTS

The summer-time fronts between stratified and tidally mixed water on the continental shelf form an important class of shallow sea fronts in many places. Although their location can usually be rationalized by using the energetic criterion of Simpson & Hunter (1974), we lack a coherent physical theory that can quantitatively account for their development and the circulation associated with them.

Ideally one would like to solve a model for the interdependent evolution of the density field and the associated circulation in response to solar heating, and forcing by wind and tide. Quite

apart from the effort required for a numerical solution of such a model, it would be very sensitive to the parametrization of the turbulent transfer of density and momentum. While numerous formulae, or modelling techniques, exist for these fluxes, they differ greatly and are particularly uncertain in stratified conditions (see Rodi (1980) for a recent review and discussion). Moreover, the mixing formulae that have been developed have usually been calibrated by applying models to estuarine situations, where vertical transfers could well be partly associated with boundary mixing and lateral intrusion as well as with local vertical transfers.

Although a coupled model for the evolution of both the stratification and circulation of a tidal mixing front appears not to have been developed yet, James (1977) has reported a vertical diffusion model in which parameters describing the eddy diffusivity and its reduction by stratification were adjusted to allow the model to explain the seasonal evolution of the temperature profile at four locations straddling a tidal mixing front in the Celtic Sea.

In a later paper James (1978) has computed the flow field associated with the density front modelled in his 1977 paper, assuming depth-dependent forms for the eddy viscosity and its reduction by stratification. His results were particularly useful in demonstrating the qualitative aspects of the circulation to be expected in the plane normal to the front, with a two-cell circulation giving surface convergence at the front. James (1978) also used his model to demonstrate the negligible role played by the advective terms in the momentum equation. However, the strength of the cross-frontal flow remains uncertain owing to the uncertainty in the basic parametrization of the Reynolds stresses. Moreover, it is easy to check that the strength of the circulation computed by James (1978) is such that the advective terms in the temperature equation, $u \partial T / \partial x + w \partial T / \partial z$, are larger in the neighbourhood of the front than the terms $\partial T / \partial t$ and $\partial(K_{\nabla} \partial T / \partial z) / \partial z$ that were equated in the earlier model. This suggests either that the cross-frontal flow has been overestimated, or that the vertical diffusivity of heat in the frontal region has been underestimated. This problem does appear to stress the need for a coupled model of cross-frontal flow and thermocline development, as well as the need for further observations.

Another 'diagnostic' model for the circulation to be expected at a tidal mixing front has been developed by Loder (1980), motivated by oceanographic observations in the Georges Bank area of the Gulf of Maine in the western North Atlantic (figures 2 and 3). The well mixed nature of the water over Georges Bank throughout the year is compatible (Garrett *et al.* 1978) with the criterion of Simpson & Hunter (1974), but estimates of the flow in the front are required to check the extent to which the observed anticyclonic flow around the bank is associated with the front, and also to estimate the cross-frontal fluxes of water properties onto the bank.

4.1. *A semi-analytic diagnostic model*

Given a prescribed density field $\rho(x, z)$, Loder (1980) calculates the horizontal velocity field implied by the governing equations

$$-fv + \rho^{-1} \partial p / \partial x = \partial(A_{\nabla} \partial u / \partial z) / \partial z, \quad (4.1)$$

$$fu = \partial(A_{\nabla} \partial v / \partial z) / \partial z, \quad (4.2)$$

$$\rho^{-1} \partial p / \partial z + g = 0. \quad (4.3)$$

The equations are the same as those used by James (1978), but with the neglect of the advective terms (which James found to be negligible; over the sloping sides of Georges Bank the term $w \partial v / \partial z$ should, perhaps, not be left out of (4.2)). The pressure is determined by the hydrostatic

equation, and horizontal mixing of momentum, found by James (1978) to be fairly unimportant even with a large horizontal eddy viscosity, is ignored.

If the viscous term on the right-hand side of (4.1) is also neglected, our earlier equation (3.7) for u follows. Leaving the viscous term in (4.1) enables us to check the accuracy of (3.7) and the role of top and bottom Ekman layers.

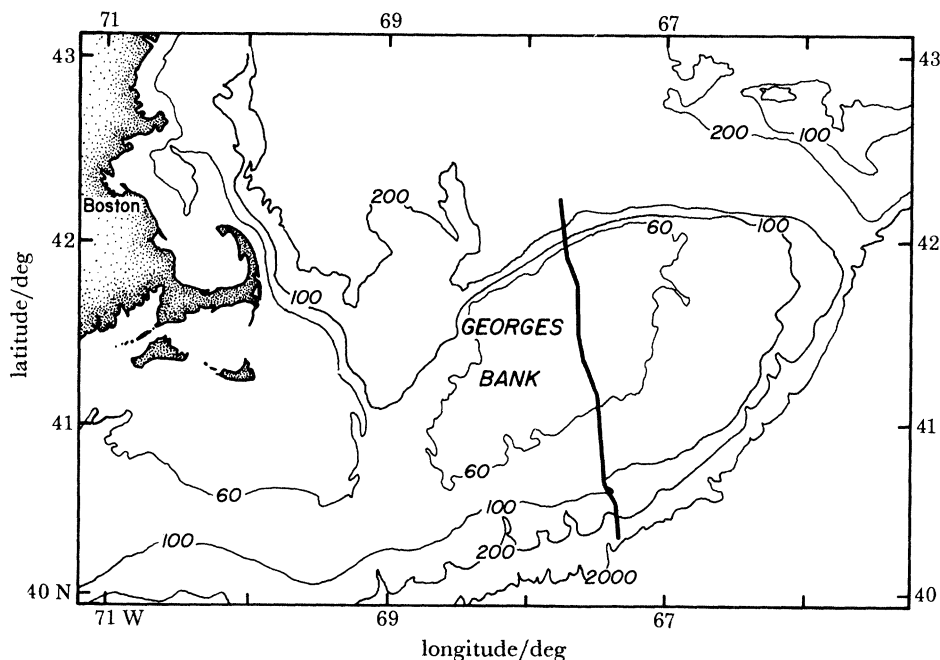


FIGURE 2. The Georges Bank region of the Gulf of Maine in the western North Atlantic, with depths in metres. The bold line indicates the location of the density section shown in figure 3.

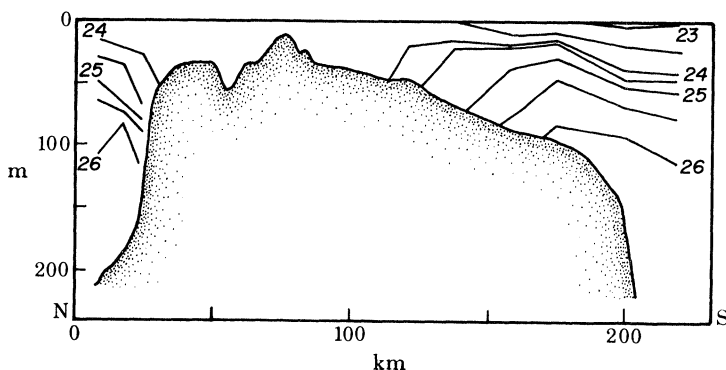


FIGURE 3. Density section (with contours in σ_t), for the line shown in figure 2, in August 1976 (redrawn from Limeburner *et al.* (1978)).

The cross-frontal pressure gradient is due to the horizontal density gradient and the sea-surface slope, which is adjusted (as in James 1978) to give zero net cross-frontal volume flux. The stress $A_{\nabla}(\partial u/\partial z, \partial v/\partial z)$ is taken to be zero at the surface $z = 0$. At the bottom, or rather at the top of the constant stress layer at $z = -h$, it is equated to a bottom stress $k(u, v)$ linearized about the tidal current. We note that these conditions imply, on integration of (4.2) from $z = -h$ to $z = 0$, that $v = \partial v/\partial z = 0$ at $z = -h$.

The eddy viscosity A_V is taken to be independent of depth (above the constant stress layer), and given by

$$A_V = A_0 F(\overline{Ri}), \quad (4.4)$$

where A_0 is the eddy viscosity in homogeneous water and $F(\overline{Ri})$ is a reducing factor depending on some average Richardson number \overline{Ri} .

Following Csanady (1976) we take

$$A_0 = \begin{cases} u_* h/20 & \text{for } h < 0.1u_*/f \\ u_*^2/200f & \text{for } h > 0.1u_*/f, \end{cases} \quad (4.5)$$

where u_* is the average friction velocity for the tidal current; i.e. $u_* = C_D^{1/2} \overline{U}_t$ with C_D a bottom drag coefficient, taken to be 2.5×10^{-3} , and \overline{U}_t the r.m.s. tidal current. The bottom friction coefficient $k = C_D \overline{U}_t$. We note that for a typical situation with $\overline{U}_t = 0.5 \text{ m s}^{-1}$ and $f = 10^{-4} \text{ s}^{-1}$, $0.1u_*/f$ is only 25 m so that for most problems we must take $A_0 = u_*^2/200f$.

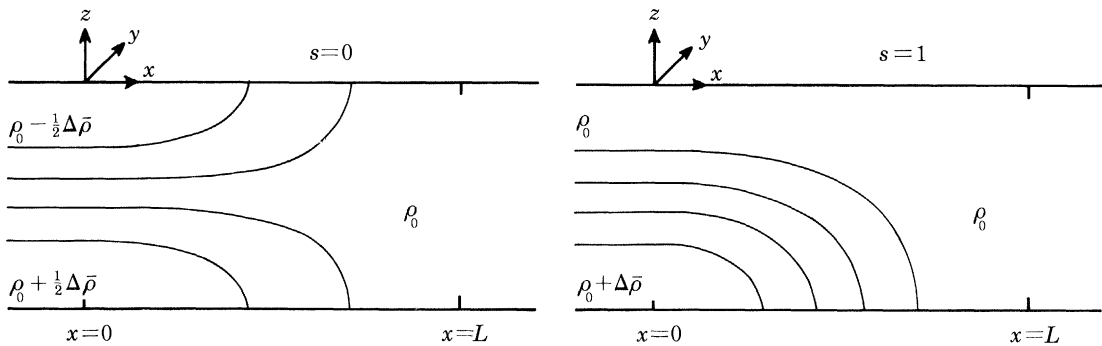


FIGURE 4. Isopycnals for $s = 0$ and $s = 1$ for the class of fronts described by equations (4.8), (4.9).

The average Richardson number is taken as

$$\overline{Ri} = g(\Delta\rho/\rho_0) h/\overline{U}_t^2, \quad (4.6)$$

with $\Delta\rho$ the change in density over the depth h , and we use the Bowden & Hamilton (1975) formula

$$F(\overline{Ri}) = (1 + 7\overline{Ri})^{-1/4}. \quad (4.7)$$

Loder (1980) has used this model to evaluate (u, v) for a distribution of horizontal density gradient given by

$$\frac{\partial\rho}{\partial x} = \frac{1}{2} \frac{\partial\Delta\rho(x)}{\partial x} \{s - \cos[\pi z/h(x)]\}. \quad (4.8)$$

With h constant and

$$\Delta\rho(x) = \begin{cases} \Delta\bar{\rho}, & x \leq 0, \\ \frac{1}{2}\Delta\bar{\rho}[1 + \cos(\pi x/L)], & 0 \leq x \leq L, \\ 0, & x \geq L, \end{cases} \quad (4.9)$$

the model represents a tidal mixing front with a surface to bottom density difference $\Delta\bar{\rho}$ on its stratified side and a cross-frontal difference of $\frac{1}{2}s\Delta\bar{\rho}$ in the depth-averaged density. For $s = 0$ and $s = 1$, the density structures are shown in figure 4.

Other forms of $h(x)$ and $\Delta\rho(x)$ can be used in (4.8). The density structure in figure 10 is for

$$h(x) = h_0 + ax \quad (4.10)$$

and

$$\Delta\rho(x) = \Delta\bar{\rho}(1 - x/L), \quad (4.11)$$

where a is the (constant) bottom slope. With variable h , $\frac{1}{2}\Delta\bar{\rho}(1-s)$ is just the cross-frontal difference in surface density.

The two critical dimensionless parameters affecting the circulation are s and an Ekman number E , defined by $A_V(fh^2)^{-1}$, which varies with x . (We ignore a weak dependence of the solutions on a third dimensionless parameter, $A_V(kh)^{-1}$, associated with the bottom boundary condition.) Figures 5–7 show profiles of u and v , with the vertical coordinate non-dimensionalized by the depth h , and the velocity non-dimensionalized by the speed $-\frac{1}{2}gh(\rho_0f)^{-1}\partial(\Delta\rho)/\partial x$ that would be achieved at the surface in the y -direction with zero friction, $s = 1$, and $v = 0$ at $z = -h$. Figure 7 shows that this is nearly achieved at the surface for $s = 1$ and very small Ekman numbers, whereas figures 5–7 together emphasize the need for a cross-frontal gradient in mean density, as well as a small Ekman number, if a significant surface flow is to be achieved.

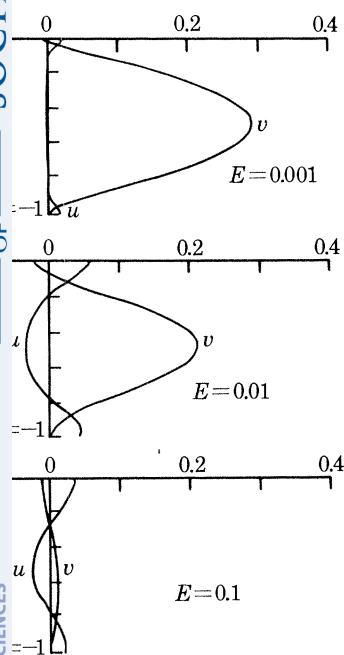


FIGURE 5. Profiles of u, v for a front with $s = 0$ and E -values as shown.

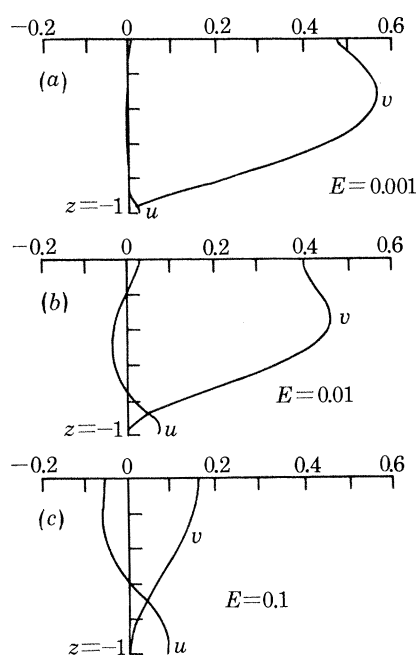


FIGURE 6. Profiles of u, v for a front with $s = 0.5$ and E -values as shown.

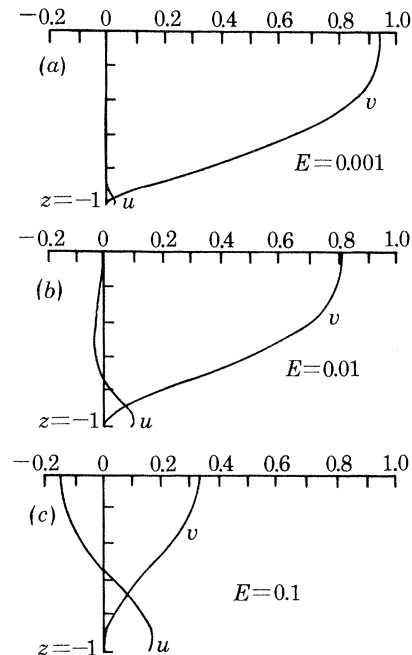


FIGURE 7. Profiles of u, v for a front with $s = 1$ and E -values as shown.

The cross-frontal flow, u , is small if E is small. In fact our equation (3.7) predicts a dimensionless value of $E\pi \sin \pi z$ which should be valid away from top and bottom Ekman layers (with thicknesses of order $(2E)^{\frac{1}{2}}h$). Figure 8 shows that the mid-depth value of u compares well with $-E\pi$ for E less than about 0.02. We note that, for the particular density chosen, u from (3.7) is negative throughout the water column, necessarily requiring a compensating positive flow in top and bottom Ekman layers.

A cross-frontal circulation pattern can be obtained from this model by prescribing E as a function of x , with E increasing towards the well mixed side of the front owing to the reduced Richardson number, the (generally) larger u_* and hence A_0 , and the smaller h (if depth variations are included). One interesting consequence of the model is shown in figure 9. A surface stagnation point ($u = 0$ at $z = 0$) is only achieved within the frontal region for large enough s and E .

4.2. Application to particular fronts

The particular density structure represented by (4.8) and (4.9) cannot be matched precisely to the Celtic Sea front investigated by James (1978), but a reasonable fit is obtained with $\Delta\bar{\rho} = 1.2 \text{ kg m}^{-3}$, $s = 0.5$, $L = 25 \text{ km}$ and $h = 95 \text{ m}$. With mean tidal current strengths from James (1977) our model gives $A_{\nabla} \approx 10^{-2} \text{ m}^2 \text{ s}^{-1}$ (reduced by 0.4 from A_0) on the stratified side of the front, and $A_{\nabla} \approx 10^{-1} \text{ m}^2 \text{ s}^{-1}$ on the mixed side. The Ekman number increases across the front from 0.01 to 0.1. The circulation predicted by the model is then very similar to that computed by James (1978), with a maximum surface speed along the front of about 0.12 m s^{-1} and a two-cell cross-frontal circulation pattern with maximum horizontal speeds of about 0.03 m s^{-1} .

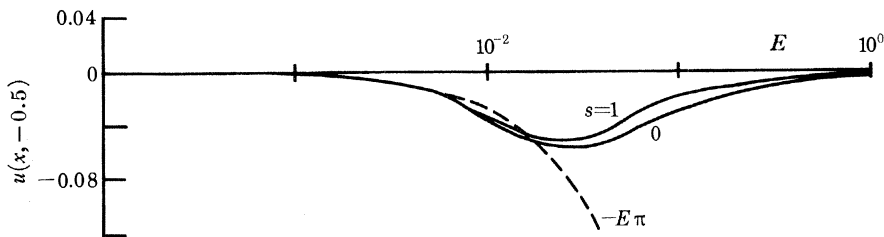


FIGURE 8. The non-dimensionalized mid-depth cross-frontal current $u(x, -0.5)$ as a function of the Ekman number E for $s = 0$ and $s = 1$. The dashed line is the low Ekman number asymptotic value $-E\pi$.

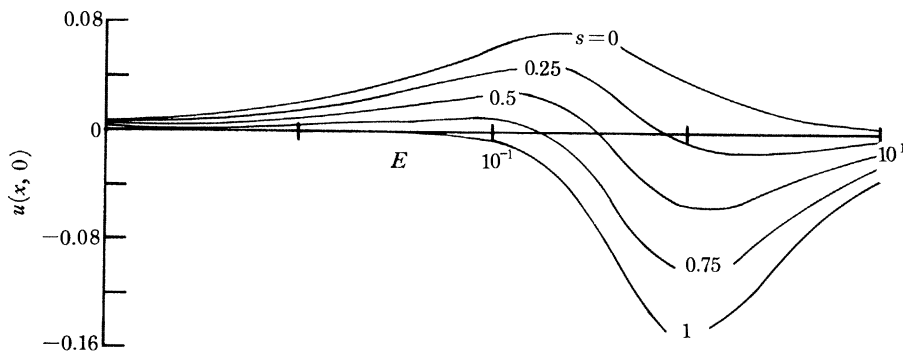


FIGURE 9. The non-dimensionalized surface cross-frontal current $u(x, 0)$ as a function of E for various values of s .

Good quantitative agreement for the surface speed along the front is not surprising. For low Ekman numbers the interior thermal wind equation (3.1) holds and the boundary condition $v = 0$ at the top of the constant stress layer, implied by zero net cross-frontal volume flux, will not change much through a thin bottom Ekman layer.

Qualitative agreement in the cross-frontal flow is also to be expected, as any form of internal friction allows water of a given density to seek its own level. Reasonable quantitative agreement, however, is surprising in view of the very different assumptions made about A_{∇} and its depth-dependence.

Figure 10 shows the streamlines for the cross-frontal flow with $s = 0.5$, and $h(x)$ and $\Delta\rho(x)$ chosen, by using (4.10) and (4.11), to approximate the front observed on the south side of Georges Bank (figure 3). The r.m.s. tidal currents, taken from Greenberg's (1979) numerical tidal model, result in ranges of $2.0 \times 10^{-3} \text{ m}^2 \text{ s}^{-1}$ to $3.7 \times 10^{-2} \text{ m}^2 \text{ s}^{-1}$ for A_{∇} across the front, 45 to 0 for Ri , and 0.002 to 0.2 for E . The two-cell circulation pattern, which we have discussed earlier,

is very evident, and is likely to be qualitatively correct even if the uncertainties in any parametrization of vertical momentum transfer reduce one's confidence in the magnitude of the computed currents. We note, in particular, a tendency for dense (cold) water to be upwelled on the well mixed side of the front, as shown in the observations of Simpson *et al.* (1978).

The extent to which this circulation pattern is associated with the maintenance, or slow evolution, of the frontal structure is uncertain. As remarked earlier, the computed cross-frontal circulation generally gives rise to advective changes in density or temperature at least as large as those assumed in a local model in which surface heating and vertical mixing are the only processes, and will certainly lead to a sharpening of horizontal gradients in the surface convergence region until, perhaps, some new balance is achieved. It is quite possible that such a balance will include processes other than those of advection and vertical diffusion admitted so far, one candidate being shear dispersion associated with oscillatory cross-frontal tidal flow.

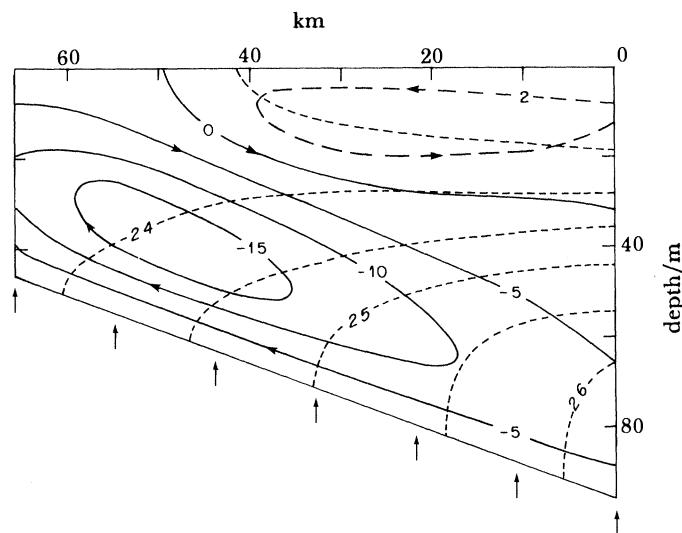


FIGURE 10. Streamlines (— and - - -) of the cross-frontal flow from application of the model to an approximation of part of the density section in figure 3. Streamfunction values are given in $10^{-2} \text{ m}^2 \text{ s}^{-1}$ and isopycnals (- - -) in σ_t units. The density difference $\Delta\bar{\rho}$ is 3.2 kg m^{-3}

Shear dispersion, and other processes that lead to cross-frontal transfer of water properties, will be discussed in more detail in the next section, but the mention of oscillatory cross-frontal flows raises another problem that deserves mention, namely the interrelation of Eulerian and Lagrangian descriptions of the flow. So far we have implicitly assumed that the density structure at a fixed point is the average over a tidal cycle, and that vertical transfers can be parametrized in terms of this density structure. However, if the width of a front is not much greater than the cross-frontal tidal excursion this approach is clearly dubious. For a model that did not attempt to resolve tidal frequencies it would be preferable to describe the density field and calculate flows in a frame of reference moving with the depth-averaged cross-frontal tidal current. In the development of a numerical model of a narrow front it would seem sensible to resolve changes at tidal frequencies, leaving just the effects of higher frequency transfers to be parametrized.

5. MECHANISMS FOR CROSS-FRONTAL TRANSFER

The location of a tidal mixing front is usually well determined by strong horizontal gradients of $\text{depth}/(\text{tidal current})^3$, as indicated by the success of Simpson & Hunter's (1974) criterion.

However, cross-frontal transfers of water properties can occur, possibly modifying the structure and properties of the water on each side of the front. In this section we shall examine the relative importance of cross-frontal transfer by the mean flow discussed in §§ 3 and 4, by horizontal shear dispersion, by baroclinic eddies and by wind.

5.1. Mean flow flux

For low Ekman number fronts the cross-frontal flow outside top and bottom Ekman layers is given by $u(x, z)$ from (3.7), so that the associated flux of a water property $C(x, z)$ is given by the integral over depth of uC . We must add to this any flux in top and bottom Ekman layers, which must exist to give zero net volume flux across the front. The relative contributions of top and bottom Ekman layers can be estimated quite simply by using the conditions $A_{\nabla} \partial v / \partial z = 0$ at $z = 0$ and $z = -h$, the latter condition being related to the need for zero net cross-frontal volume flux (see § 4.1). Hence the net cross-frontal flux due to the mean flow (denoted by $F_{m.f.}$) may be written for low Ekman number as

$$F_{m.f.} = - \int_{-h}^0 g f^{-2} \rho^{-1} (A_{\nabla} \rho_x)_z C \, dz + g f^{-2} \rho^{-1} [A_{\nabla} \rho_x C]_{-h}^0 \quad (5.1)$$

$$= \int_{-h}^0 g f^{-2} \rho^{-1} A_{\nabla} \rho_x C_z \, dz. \quad (5.2)$$

Calculations with the model described in § 4.1 indicate that (5.2) gives accurate answers for the mass flux (putting $C = \rho$) for Ekman numbers up to about 0.03, but overestimates the net mass flux by a factor of 2 when $E = 0.1$.

We note that the mean flow flux of mass given by (5.2) may be written as

$$F_{m.f.} = - \int_{-h}^0 (N^2/f^2) A_{\nabla} \rho_x \, dz. \quad (5.3)$$

This is the same as if it were given by the depth-dependent horizontal diffusivity $(N^2/f^2) A_{\nabla}$ that describes the advective evolution of isopycnals in the fluid interior, as described in § 3.

We note that the mean flow flux of mass is a function of the cross-frontal coordinate x , with the maximum value occurring in the front. The divergence in this flux can perhaps be balanced by other horizontal mixing processes on the well mixed side of a tidal mixing front, but will lead to a progressive decrease in the depth-averaged density on the stratified side of a front in the typical situation were the average density is less on the well mixed than on the stratified side of the front. However, before reaching any definite conclusions we must compare the mean flow flux with other horizontal exchange processes.

If there is some other process that can be parametrized by some horizontal diffusivity K_H acting on the depth-averaged horizontal gradient of C , then the horizontal mixing flux ($F_{h.m.}$) is $K_H \int_{-h}^0 C_x \, dz$. Thus for the mass flux the ratio $F_{m.f.}/F_{h.m.}$ can be estimated by $(N^2/f^2) (A_{\nabla}/K_H)$. We next examine values of K_H appropriate to the well known mechanism of shear dispersion.

5.2. Shear dispersion

Shear dispersion describes the lateral spreading of a substance due to a combination of vertical shear of the horizontal current and vertical mixing. The topic is reviewed by Fischer *et al.* (1979) who also discuss the case of oscillatory flow that is relevant to the present problem, where significant vertical shears of oscillatory cross-frontal flows are possible, associated with tidal currents, inertial oscillations or wind-induced flows.

A significant factor in the effectiveness of shear dispersion in an oscillatory flow is the ratio T/T_c of the period T of the flow to the time T_c required for mixing over the depth of the fluid. If $T/T_c \ll 1$, then a vertical dye streak would merely oscillate about its mean position without as much chance for vertical mixing to produce a net horizontal transfer as for $T/T_c \gg 1$. Fischer *et al.* (1979) have shown that the horizontal diffusivity K_H due to shear dispersion is independent of T/T_c for $T/T_c \gg 1$ (where $T_c = h^2/K_V$), but reduced for small values of T/T_c . For a linear velocity profile and constant K_V they found a reduction factor of $3(T/T_c)^2$ for $T/T_c < 0.2$.

In fact it is easy to show by simple geometrical arguments that for $T/T_c \ll 1$

$$K_H = (S^2/\omega^2) K_V, \quad (5.4)$$

where S^2 is the mean-square vertical shear of the horizontal current which oscillates with frequency ω . This value of K_H applies at any depth provided that h in $T_c = h^2/K_V$ is replaced by the vertical scale of the shear. (Equation (5.4) may be verified for a particular velocity profile by examining equation (4.55) of Fischer *et al.* (1979).)

If $T/T_c \gtrsim 1$ the value of K_H depends on the details of the oscillatory current profile as well as on K_V . Bowden (1965) computed K_H/u_*h for several current profiles (where u_* is the friction velocity and he took $K_V \approx 0.06u_*h$) finding values between 6 and 25. If $K_V = u_*^2/200f$, as discussed in § 4, the appropriate value of K_H needs to be evaluated properly, but if $K_H \propto K_V^{-1}$ for $T/T_c > 1$ (Fisher *et al.* 1979), then from Bowden's (1965) results we might expect $K_H \approx 200fh^2$.

If we take $u_*^2/200f$ from (4.5) as an upper bound for K_V , not allowing for a reduction by stratification, then the condition $T/T_c < 0.2$ reduces to the requirement that the r.m.s. tidal current \bar{U}_t be less than $50(f\omega)^{1/2}h$. For $f = 10^{-4} \text{ s}^{-1}$ and $\omega = 1.4 \times 10^{-4} \text{ s}^{-1}$, appropriate to M_2 , this becomes $\bar{U}_t < 0.3 \text{ m s}^{-1}$ if we take $h = 50 \text{ m}$. The condition $T/T_c > 1$ would require $\bar{U}_t > 0.7 \text{ m s}^{-1}$. As K_V will be substantially reduced by stratification, the formula (5.4) seems to be the appropriate one to use in the front. The ratio of the mean flow flux to the shear dispersion flux ($F_{s.d.}$) of mass across the front is then

$$F_{m.f.}/F_{s.d.} \approx (N^2/f^2) (\omega^2/S^2) (A_V/K_V) \quad (5.5)$$

$$= (N^2/S^2) (\omega^2/f^2) Pr, \quad (5.6)$$

where Pr is the eddy Prandtl number.

As the Richardson number N^2/S^2 for the oscillatory flow is likely to be of order 1 or more, and $\omega^2/f^2 = 2$ for M_2 tides at mid-latitudes and 1 for inertial oscillations, the ratio $F_{m.f.}/F_{s.d.}$ depends mainly on the eddy Prandtl number, which is usually assumed to be large in stratified conditions. We conclude that the cross-frontal flux associated with the mean flow is likely to be significantly greater than that due to shear dispersion associated with either inertial oscillations or tides. However, it is possible that low frequency wind-induced cross-frontal excursions could lead to a greater importance of shear dispersion if $T > T_c$, for which $F_{m.f.}/F_{s.d.} \approx (N^2/f^2) A_V/(200fh^2)$. Also, even if the mean flow flux appears to be greater than the shear dispersion flux at tidal frequencies, the tidal oscillations may produce periods each tidal cycle during which the vertical density gradient is reduced (Allen *et al.* 1980), vertical mixing enhanced, and so the mean flow flux greater than it would be without cross-frontal tidal excursions.

The comparison of the mean flow flux and the shear dispersion flux in (5.5) refers to the depth-integrated values of the mass flux. While it suggests that the shear dispersion associated with tidal and inertial oscillations is not important for the net mass flux, it is quite possible that horizontal shear dispersion plays an important role in the evolution of the density field at some depths.

Moreover, it is clear from the above discussion that the shear dispersion flux is of increasing relative importance as the well mixed side of the front is approached, and could there, perhaps, pick up part of the flux that is carried by the mean flow within the front.

5.3. Barotropic eddies

In tidally energetic shallow seas the horizontal mixing coefficient K_H generally seems to be much greater than that attributable to shear dispersion. Zimmerman (1976) has shown how oscillatory tidal excursions in a field of barotropic residual eddies, which may themselves be generated by tidal flow over bottom topography or past prominent coastal features (Zimmerman 1978), can lead to values of K_H up to $10^3 \text{ m}^2 \text{ s}^{-1}$. Clearly a value this large can be greater than the effective $A_V N^2/f^2$ due to the mean flow flux in § 5.1, but further work is required to establish the local value of K_H associated with this mechanism in any particular frontal region.

5.4. Baroclinic eddies

Most fronts on the continental shelf show significant low frequency eddy activity with a horizontal scale of order 10 km. It is usually assumed that the eddies arise from baroclinic instability of the frontal jet, and it is suspected that they play an important role in cross-frontal transfer. Pingree (1978, 1979) has examined the problem for various fronts in the Celtic Sea and other areas of the northwest European continental shelf, and used Green's (1970) formula for poleward heat transfer in the atmosphere to make an estimate of the cross-frontal heat flux for continental shelf fronts. Our main purpose here is to compare Pingree's (1979) estimate of the flux due to baroclinic eddies with our estimate of the cross-frontal flux associated with the mean flow.

We envisage a front like that shown in figure 3 on the south side of Georges Bank. For such a front (with $0 < s < 1$ in the context of our model in § 4), the mean flow across it tends to move light water onto the bank near the surface, dense water onto the bank near the bottom, and water of intermediate density off the bank at mid-depth. The net effect depends on the vertical structure of A_V (see equation (5.3)), but probably tends to increase the density of water on the bank.

Calculations for a three-layer model, with isopycnal and bottom slopes similar to those shown in figure 3, indicate two modes of baroclinic instability, one largely associated with each interface (Wright 1978). Bottom friction is likely to prevent growth of the deeper mode, so we assume that eddies generated by baroclinic instability are confined to the upper part of the water column from the surface to, say, the depth D at which the horizontal density gradient vanishes (although further theoretical and observational work is clearly required to check this). Following Pingree (1979) we then estimate the net baroclinic eddy flux ($F_{b.e.}$) of mass off the bank to be

$$F_{b.e.} = \alpha(g'D)^{\frac{1}{2}} \left(\frac{1}{2}\Delta\rho_s\right) D. \quad (5.7)$$

Here $\Delta\rho_s$ is the surface density difference across the front and $(g'D)^{\frac{1}{2}}$, with $g' = g\Delta\rho_s/\rho_0$, is the maximum speed that could result from potential energy release. The coefficient α is a dimensionless multiplier which Pingree takes to be 0.0055, following Green (1970), and we have taken $\frac{1}{2}\Delta\rho_s$ as the average density difference across the front between the surface and depth D .

We compare $F_{b.e.}$ not with the mean flow flux over the whole depth (which, as mentioned, is likely to have the opposite sign), but rather with the flux associated with the surface Ekman layer and whatever depth is required for a compensating volume flux. The net mass flux for this part of the mean flow is then

$$F_{m.f.} \approx gf^{-2}\rho^{-1}A_V(\partial\rho/\partial x) \left(\frac{1}{2}\Delta\rho_s\right), \quad (5.8)$$

where $\partial\rho/\partial x$ is the surface density gradient, which we take as $\Delta\rho_s/L_s$, with L_s the horizontal scale of the front. The ratio of mean flow flux to baroclinic eddy flux may then be written

$$F_{m.f.}/F_{b.e.} = A_V(fD^2)^{-1}\alpha^{-1}(L_R/L_s), \quad (5.9)$$

where L_R is the internal Rossby radius of deformation $(g'D)^{1/2}/f$. A typical value of $\Delta\rho_s$ for the tidal mixing fronts in the Gulf of Maine is 0.5 kg m^{-3} , and $D \approx 20\text{ m}$, so $L_R \approx 3\text{ km}$ for $f = 10^4\text{ s}^{-1}$. Then with $A_V \approx 10^{-2}\text{ m}^2\text{ s}^{-1}$ in the centre of the front, $\alpha = 0.0055$ and $L_s \approx 20\text{ km}$ we have $F_{m.f.}/F_{b.e.} \approx 7$, so that the baroclinic eddy flux appears to be less important than that associated with the mean flow. However, we must remember that the mean flow flux varies across the front, so that other processes are required to maintain a balance.

The estimates above are critically dependent on the values of A_V and α as well as on our assumption about the depth of the baroclinic zone. The parameter α may be interpreted in terms of the time T_e between the exchange across the front of circular rings of fluid of radius R , with two rings requiring a distance $4R$ along the front. Assuming again that only a depth D is affected and that the exchanged water parcels have average densities that differ by $\frac{1}{2}\Delta\rho_s$ gives a net mass flux

$$F_{b.e.} = \pi R^2(\frac{1}{2}\Delta\rho_s) D(4R)^{-1} T_e^{-1}. \quad (5.10)$$

Equating this to (5.7) gives

$$\alpha = \frac{1}{8}(R/L_R) (T_i/T_e) \quad (5.11)$$

where $L_R = (g'D)^{1/2}/f$ is, as before, the Rossby radius based on $\Delta\rho_s$ and D , and $T_i = 2\pi f^{-1}$ is the inertial period.

Observations of eddies in infrared imagery of the fronts around Georges Bank suggest $R \approx 5L_R$ (possibly closer to a Rossby scale based on the total depth), so for $\alpha = 0.0055$ we require eddies to form and cross the front about every 80 days. Even after allowance has been made for spatial as well as temporal intermittency, preliminary examination of infrared images suggests that eddies may be slightly more frequent than this, so that (5.7) slightly underestimates the cross frontal mass flux. Moreover, the vertical eddy viscosity used in evaluating the mean flow flux, while obtained from existing formulae, may well turn out eventually to be an overestimate.

It is quite possible that baroclinic eddies are the major factor in cross-frontal transfers, though, of course, smaller scale mixing is still required if the eddies are to merge into their new surroundings. We also point out that eddy formation stretches a front and so is presumably associated with lateral convergence which may play a role in frontal maintenance.

5.5. Wind-driven transfer

We must also consider the possibility that the dominant cross-frontal transfer of water properties is associated with a steady, or low-frequency, cross-frontal flow due to surface wind stress. As an example let us consider a wind stress τ parallel to the front, producing a cross-frontal Ekman flux $\tau/\rho f$. Assuming that a return flow is set up, and that the two flows differ in average density by $\frac{1}{2}\Delta\rho_s$, i.e. half the surface density difference across the front, the wind-driven flux ($F_{w.d.}$) of mass is

$$F_{w.d.} = \tau\rho^{-1}f^{-1}(\frac{1}{2}\Delta\rho_s). \quad (5.12)$$

Comparing this with the partial mean flow flux, as defined in (5.8), we obtain

$$F_{m.f.}/F_{w.d.} = gf^{-1}A_V(\partial\rho/\partial x) \tau^{-1}. \quad (5.13)$$

Taking, as in § 5.4, $A_V = 10^{-2} \text{ m}^2 \text{ s}^{-1}$ and $\partial\rho/\partial x \approx 0.5 \text{ kg m}^{-3}/20 \text{ km}$ we see that for the wind driven flux to be comparable with the mean flow flux requires a wind stress of only 0.025 Pa, and hence an average wind of only about 4 m s^{-1} . However, this comparison ignores the rest of the mean flow flux (§ 5.1) which could be greater.

Further work on this is obviously required, particularly allowing for time-dependent winds and relating the above estimate to the discussion of shear dispersion in § 5.2. Also, the increased vertical mixing on the well mixed side of a tidal mixing front will tend to produce a flow more nearly parallel to the wind than on the stratified side of the front (Hopkins & Garfield 1979). This raises interesting possibilities for surface convergence at the front.

5.6. Summary

A comparison of five mechanisms for cross-frontal transfer suggests the dominance of the flux associated with the frictionally induced mean flow, at least for typical tidal mixing fronts and existing parametrizations of vertical mixing, although it could be exceeded by dispersion due to tidal excursions in barotropic residual eddies over topography. The net horizontal transfer by shear dispersion in inertial and tidal oscillations is likely to be less than the mean flow flux provided only that the eddy Prandtl number in a stratified fluid is large. The transfer by baroclinic eddies appears to be less than the mean flow flux in mid-front, but this conclusion could easily change if it turns out that existing formulae overestimate A_V . A factor that may be as important as any other is the wind stress parallel to the front.

Observations of cross-frontal eddy fluxes of water properties are clearly required. The frequency dependence of cross-spectra of the cross-frontal velocity component and, say, density, at a number of depths and lateral positions should provide useful clues on cross-frontal transfer mechanisms. However, careful distinction between Eulerian and Lagrangian, or semi-Lagrangian, estimates will be required. It is possible, for example, that one would find a peak at the tidal frequency in the cross-spectrum of Eulerian variables, giving the impression of shear dispersion even though the flux might be more sensibly thought of as a mean flow flux in a frame of reference moving normal to the front with the depth-averaged tidal current.

One process for cross-frontal transfer that has not been discussed is the large-scale entrainment by eddies generated elsewhere. The process is clearly important for an area like Georges Bank which can be greatly influenced by Gulf Stream rings, but requires separate discussion for each situation, rather than lending itself to the fairly general description we have given to other processes.

6. DISCUSSION

The main thrust of this paper has been to examine the role of internal friction in the evolution of an oceanic front. Application of the general results on cross-frontal flow derived in § 3 shows that, with existing parametrizations of vertical mixing of momentum on the continental shelves, the frictionally induced cross-frontal flow makes an important contribution to the local density balance in a tidal mixing front, and appears to dominate shear dispersion and baroclinic eddies in producing cross-frontal transfer. This cross-frontal flow, which basically describes the tendency of fluid to seek its own level if the constraint of geostrophy is broken by friction, tends to lead to an increase of horizontal gradients on the mixed side of a tidal mixing front, but further work with a coupled model of thermocline development, including horizontal

advection as well as vertical mixing, is required for an investigation of the development and structure of a front.

The results described in this paper are clearly very sensitive to the parametrization of vertical momentum mixing in terms of factors such as tidal current, water depth and stratification. In stratified conditions in particular existing formulae are very uncertain. Our own suspicion is that they tend to overestimate the mixing rates, but clearly much more work involving inference from observations of the mean flow and direct eddy flux measurement is required.

Our work has been supported by the Natural Science and Engineering Research Council of Canada. Since December 1980 J. W. L. has been supported by a postdoctoral fellowship at Woods Hole Oceanographic Institution. We thank Dan Wright for discussions on several of the topics treated in this paper, and Barbara-Ann Juszko for contributions to § 2.1. Phil Richardson and Bob Beardsley (W.H.O.I.) and Francis Jordan (B.I.O.) generously provided access to their files of satellite imagery. Adrian Gill gave us helpful comments on a draft of the paper.

REFERENCES (Garrett & Loder)

- Allen, C. M., Simpson, J. H. & Carson, R. M. 1980 *Oceanologica Acta*, **3**, 59–68.
 Bowden, K. F. 1965 *J. Fluid Mech.* **21**, 83–95.
 Bowden, K. F. & Hamilton, P. 1975 *Estuar. coast. mar. Sci.* **3**, 281–301.
 Csanady, G. T. 1976 *J. geophys. Res.* **81**, 5389–5399.
 Csanady, G. T. 1978 *J. geophys. Res.* **83**, 2329–2342.
 Csanady, G. T. 1980 *J. geophys. Res.* **84**, 777–780.
 Fischer, H. B., List, E. J., Koh, R. C. Y., Imberger, J. & Brooks, N. H. 1979 *Mixing in inland and coastal waters* (483 pp.). New York: Academic Press.
 Garrett, C. & Horne, E. 1978 *J. geophys. Res.* **83**, 4651–4656.
 Garrett, C. J. R., Keeley, J. R. & Greenberg, D. A. 1978 *Atmosphere–Ocean* **16**, 403–423.
 Gill, A. E. 1981 *J. Fluid Mech.* **103**, 275–295.
 Green, J. S. A. 1970 *Q. Jl R. met. Soc.* **96**, 157–185.
 Greenberg, D. A. 1979 *Marine Geod.* **2**, 161–187.
 Hopkins, T. S. & Garfield, N. 1979 Physical characteristics of Georges Bank water. Abstract, Second Informal Workshop on the Oceanography of the Gulf of Maine and Adjacent Seas, Dalhousie University, May 1979.
 James, I. D. 1977 *Estuar. coast. mar. Sci.* **5**, 339–353.
 James, I. D. 1978 *Estuar. coast. mar. Sci.* **7**, 197–202.
 Limeburner, R., Vermersch, J. A. & Beardsley, R. C. 1978 *Tech. Rep. Woods Hole oceanogr. Instn* WHOI-78-83 (116 pp.).
 Loder, J. W. 1980 Ph.D. thesis, Dalhousie University (279 pp.).
 Pedlosky, J. 1979 *Geophysical fluid dynamics* (624 pp.). New York: Springer-Verlag.
 Pingree, R. D. 1978 *J. mar. biol. Ass. U.K.* **58**, 955–963.
 Pingree, R. D. 1979 *J. mar. biol. Ass. U.K.* **59**, 689–698.
 Rodi, W. 1980 *Lecture notes on coastal and estuarine studies*, vol. 1. *Mathematical modelling of estuarine physics* (ed. J. Sündermann & K.-P. Holz). New York: Springer-Verlag.
 Simpson, J. H. & Hunter, J. R. 1974 *Nature, Lond.* **250**, 404–406.
 Simpson, J. H., Allen, C. M. & Morris, N. C. G. 1978 *J. geophys. Res.* **83**, 4607–4614.
 Stommel, H. & Fedorov, K. N. 1967 *Tellus* **19**, 306–325.
 Tang, C. 1980 *J. geophys. Res.* **85**, 2787–2796.
 Wright, D. G. 1978 Mixed baroclinic–barotropic instability with oceanic applications. Ph.D. thesis, University of British Columbia (211 pp.).
 Zimmerman, J. T. F. 1976 *Neth. J. Sea Res.* **10**, 397–439.
 Zimmerman, J. T. F. 1978 *Geophys. astrophys. Fluid Dyn.* **11**, 35–47.